# Bifunctional $ZnMn_2O_4$/reduced graphene oxide microspheres with needle-like surface architecture as effective electrodes for energy storage

P. Rosaiah[1,2*] ,[1]Nunna Guru Prakash[2], M. Dhananjaya[2], Bandar Ali Al-Asbahid[3], Sangaraju Sambasivam[4], U.Chalapathi[5 *], Si-Hyun Park[5 *]

[1] School of Mechanical Engineering, Yeungnam University, 280 Daehak-ro, Gyoungsan-si, Gyeongsangbuk-do 38541, Republic of Korea

[2] Department of Physics, Saveetha School of Engineering, Saveetha Institute of Medical and Technical Sciences (SIMATS), Thandalam, Chennai 602 105, India.

[3] Department of Physics & Astronomy, College of Science, King Saud University, P.O. Box 2455, Riyadh 11451, Saudi Arabia

[4] National Water and Energy Center, United Arab Emirates University, Al Ain - 15551, UAE.

[5] Department of Electronic Engineering, Yeungnam University, 280 Daehak-Ro, Gyeongsan, Gyeongbuk 38541, South Korea

## EXPERIMENTAL

**Synthesis:** Graphene oxide was prepared as per our previous reports. Carbon nanospheres were first prepared by dissolving 7 g of glucose in 70 ml of water and then hydrothermally synthesized at 180 °C for 12 h. To prepare ZNMNO/RGO composites, 40 mg GO was dispersed in 120 ml ethylene glycol under proper sonification. Then, 0.9 g Zn $(CH_3COO)_2 \cdot 2H_2O$, 2.5 g Mn $(CH_3COO)_2 \cdot 2H_2O$, 0.2g Polyvinylpyrrolidone (PVP) and 1.2 g carbon spheres were added in to the above solution while continuous stirring. After 30 minutes, the mixture was transferred to 150 ml autoclave and heated @180 °C for 12 h. The resultant product was washed several times using routine protocol and dried at 80 °C overnight. The obtained powder was then calcinated in a tube furnace at 500-700 °C for 4 h under controlled $N_2$ atmosphere at a slow heating rate.

**Characterization:** The phase purity and crystal structure of the prepared samples were characterized using monochromatic high-intensity Cu Kα radiation (1.5406 Å) by the powder

* Corresponding authors. E-mail: dr.mosesrosaiah@gmail.com

X-ray Diffraction (XRD) system (MPD for bulk, 3KW, PANalytical). The morphological and elemental compositions were studied by Field Emission Scanning Electron Microscopy (FESEM, Hitachi S-4800) and Transmission Electron Microscopy (TEM; Tecnai G2 F20STwin), respectively. The surface area and pore diameter/volume of the electrodes were determined by $N_2$ adsorption–desorption isotherm measurements from an automatic surface analyzer (3 Flex, Micrometrics, USA) using BET (Brunauer-Emmett-Teller) and Barrett-Joyner-Halenda (BJH) calculations. The vibrational bands between atoms in the prepared samples were determined by Raman spectrometer (XploRA Plus, HORIBA KOREA). The oxidation states and stoichiometry of the elements in the electrode were investigated by X-ray photoelectron spectroscopy (XPS; Thermo Scientific) using Al Kα radiation under a pressure of 5×10-9 Torr.

To test the LIB performance, the resultant ZNMNO/RGO composite were made following our previous publications' standardized protocol and used as working electrodes. The cell was composed of synthesized composites as working electrode, lithium foil as counter, and reference electrode. The electrolyte was a 1:1, v/v solution of $LiPF_6$ in 1 M ethylene and dimethyl carbonates. The mass loading of the electrodes was ~2 $mg.cm^{-1}$. The separator utilized was Celgard-2400. The cells performed galvanostatic discharge/charge cycles over a potential range of 0.01 and 3.0 V on a battery tester. Cyclic voltammetry (CV) and electrochemical impedance spectroscopy (EIS) were performed on an electrochemical analyzer (Model: VERTEX).

To investigate the capacitance behavior, the ZNMNO/RGO composite samples were employed to support the working electrode. A piece of Ni-Foam (1x1.5 cm) was sliced and subjected to sequential ultrasonic cleaning in DI water, ethanol, and acetone for 1 h, which was coated by mixing the active materials of the electrode with Nafion and ethanol. The obtained

slurry was then coated on the cleaned Ni-Foam via casting and dried overnight in an oven at 80 °C. In the three-electrode system, the as-fabricated active electrodes served as working electrodes, and platinum plate and saturated calomel electrode (SCE) were used as counter electrode and reference electrode, respectively. Cyclic voltammetry (CV) tests and galvanostatic charge−discharge (GCD) tests were performed in 1 M $Na_2SO_4$ solution at a potential window ranging from 0 to 0.1V, respectively. Electrochemical impedance spectroscopy (EIS) tests were conducted in a varying frequency range of 100-0.01 Hz with alternate current amplitude of 5 mV. The specific capacitance ($C_s$) was calculated using the following equation.

$$c_s = \frac{I \times \Delta t}{m \times \Delta V}$$

Where $I$, $\Delta t$, $m$, $\Delta V$ were discharge current (A), discharge time (s), Active mass (g) and the potential window (V), respectively.

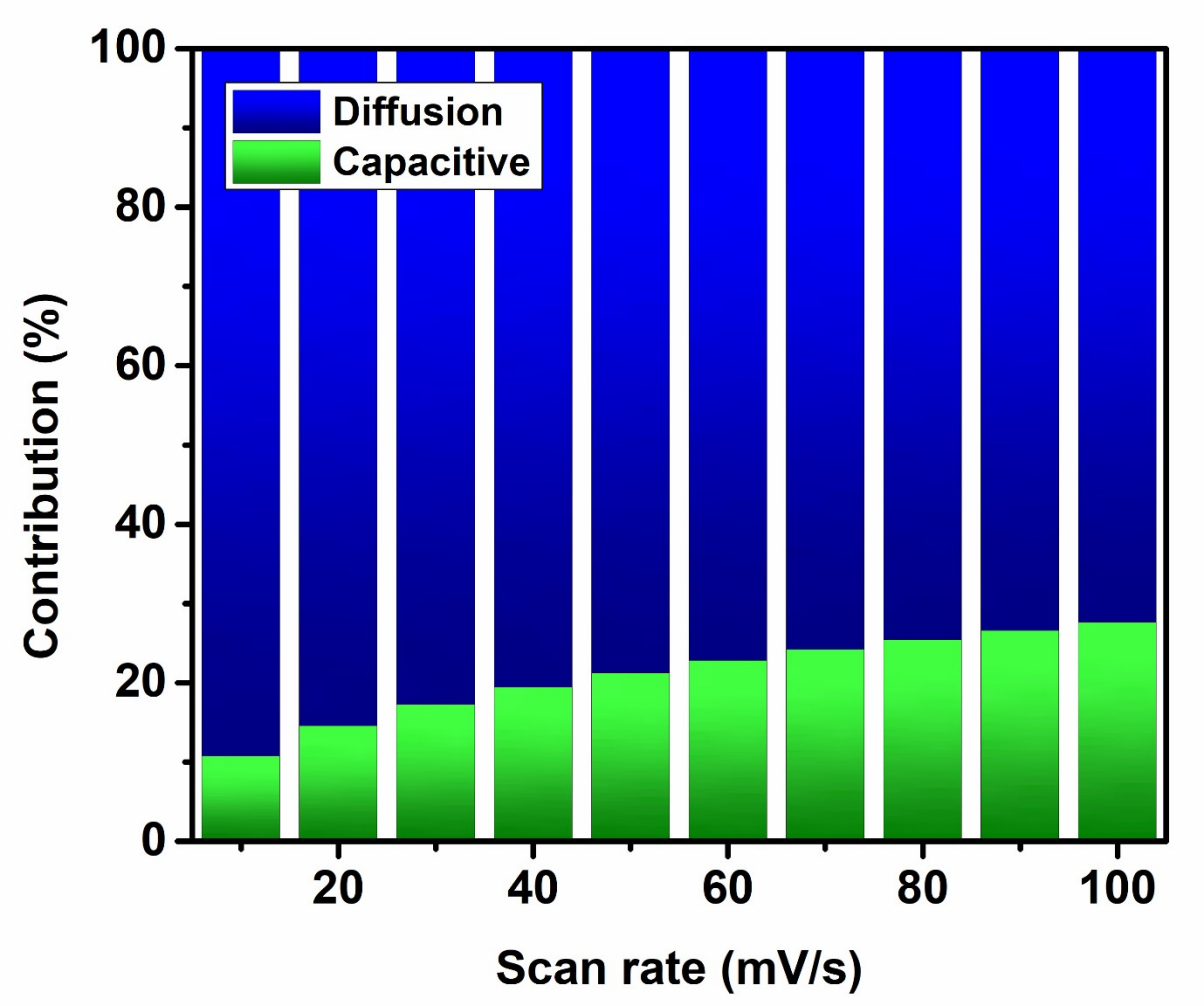


Fig.S1. capacitance contribution at different scan rates

Table S1 Literature review on electrochemical performance of $ZnMn_2O_4$ composites with different surface morphologies for Li-ion batteries

| S. No | Materials | Initial discharge/charging Capacity (mA h $g^{-1}$) | Restored Capacity (mA h $g^{-1}$) | Cycles | Current density (A $g^{-1}$) | Ref. No |
|---|---|---|---|---|---|---|
| 1 | Nanocrystalline $ZnMn_2O_4$ | 1302/766 @0.1 A/g | 569 | 50 | 0.1 | [1] |
| 2 | rGO–$ZnMn_2O_4$ composite | 1412/960 @0.1 A/g | 707 | 50 | 0.1 | [2] |
| 3 | Loaf-like $ZnMn_2O_4$ | 1357/839 @0.1 A/g | 517 | 100 | 0.5 | [3] |
| 4 | quasi-mesocrystal $ZnMn_2O_4$ | 1106/732 @0.5 A/g | 860 | 130 | 0.5 | [4] |
| 5 | Flower-like $ZnMn_2O_4$ | 763 @ 0.1 A/g | 626 | 50 | 0.1 | [5] |
| 6. | $ZnMn_2O_4$ nanoparticles | 1200/680 @C/10 | 430 | 40 | C/10 | [6] |
| 7 | Ball -in ball $ZnMn_2O_4$ | 945/662 @0.4 A/g | 490 | 50 | 0.4 | [7] |
| 8 | Sandwich $ZnMn_2O_4$ | 1559/899 @0.18 A/g | 945 | 150 | 0.18 | [8] |
| 9 | $ZnMn_2O_4$ mesocrystals | 1309/945 @ 0.1 A/g | 608 | 100 | 0.1 | [9] |
| **10** | **$ZnMn_2O_4$/RGO composites** | **1578/1012 @0.1 A/g** | **686** | **300** | **1** | **Present Work** |


[1] Y. Yang, Y. Zhao, L. Xiao, L. Zhang, Nanocrystalline ZnMn2O4 as a novel lithium-storage material, Electrochem. Commun. 10 (2008) 1117–1120. https://doi.org/10.1016/j.elecom.2008.05.026.

[2] Z. Zheng, Y. Cheng, X. Yan, R. Wang, P. Zhang, Enhanced electrochemical properties of graphene-wrapped ZnMn 2O4 nanorods for lithium-ion batteries, J. Mater. Chem. A. 2 (2014) 149–154. https://doi.org/10.1039/c3ta13511j.

[3] Z. Bai, N. Fan, C. Sun, Z. Ju, C. Guo, J. Yang, Y. Qian, Facile synthesis of loaf-like

ZnMn2O4 nanorods and their excellent performance in Li-ion batteries, Nanoscale. 5 (2013) 2442–2447. https://doi.org/10.1039/c3nr33211j.

[4] Y. Liu, J. Bai, X. Ma, J. Li, S. Xiong, Formation of quasi-mesocrystal ZnMn2O4 twin microspheres via an oriented attachment for lithium-ion batteries, J. Mater. Chem. A. 2 (2014) 14236–14244. https://doi.org/10.1039/c4ta02950j.

[5] L. Xiao, Y. Yang, J. Yin, Q. Li, L. Zhang, Low temperature synthesis of flower-like ZnMn2O4 superstructures with enhanced electrochemical lithium storage, J. Power Sources. 194 (2009) 1089–1093. https://doi.org/10.1016/j.jpowsour.2009.06.043.

[6] F.M. Courtel, Y. Abu-Lebdeh, I.J. Davidson, ZnMn2O4 nanoparticles synthesized by a hydrothermal method as an anode material for Li-ion batteries, Electrochim. Acta. 71 (2012) 123–127. https://doi.org/10.1016/j.electacta.2012.03.108.

[7] G. Zhang, L. Yu, H. Bin Wu, H.E. Hoster, X.W. Lou, Formation of ZnMn 2O 4 ball-in-ball hollow microspheres as a high-performance anode for lithium-ion batteries, Adv. Mater. 24 (2012) 4609–4613. https://doi.org/10.1002/adma.201201779.

[8] G. Gao, S. Lu, B. Dong, W. Yan, W. Wang, T. Zhao, C.Y. Lao, K. Xi, R.V. Kumar, S. Ding, Construction of sandwich-type hybrid structures by anchoring mesoporous ZnMn2O4 nanofoams on reduced graphene oxide with highly enhanced capability, J. Mater. Chem. A. 4 (2016) 10419–10424. https://doi.org/10.1039/c6ta03226e.

[9] R. Jin, Q. Wen, L. Yang, G. Li, ZnMn2O4 mesocrystals for lithium-ion batteries with high rate capacity and cycle stability, Mater. Lett. 135 (2014) 55–58. https://doi.org/10.1016/j.matlet.2014.07.132.